Hindawi Publishing Corporation
Journal of Nanomaterials
Volume 2012, Article ID 180989, 8 pages
doi:10.1155/2012/180989

Research Article

Two-Step Self-Assembly and Lyotropic Liquid Crystal Behavior of TiO_2 Nanorods

Zhimin Ren, Chao Chen, Rong Hu, Kaiguang Mai, Guodong Qian, and Zhiyu Wang

State Key Laboratory of Silicon Materials, Department of Materials Science and Engineering, Zhejiang University, Hangzhou 310027, China

Correspondence should be addressed to Zhiyu Wang, wangzhiyu@zju.edu.cn

Received 17 April 2012; Revised 10 June 2012; Accepted 25 June 2012

Academic Editor: Tianxi Liu

Several self-assembly structures of anatase TiO_2 nanorods were obtained by a two-step assembly process, and these structures formed different lyotropic liquid crystal in solution. Primary self-assembly occurred in synthesis process and formed two structures, in the morphology of ribbon and honeycomb, respectively. Secondary-assembly took place when the products were placed at lower temperature, where unique structures were obtained as the relative amount of ribbon and honeycomb changed with the increase of TiO_2 concentration. These structures showed nematic, spherulites, and lamellar phases. The mechanism of the two-step self-assembly was clarified. The driving force of primary assembly is deduced to be anisotropic attractive force, for NRs can assemble at any concentrations, while gravity is the driving force of the secondary assembly. It is worth mentioning that this paper is the first report about spherulites composing of anatase TiO_2 nanorods. The spherulites obtained were negative or of tangential type, and its structure, growth process, and temperature influences were also investigated. The spherulites may have promising application in temperature microsensor.

1. Introduction

For more than a hundred years, the new liquid crystal materials have acquired increasing attraction of scientists who focus on practical application and physical principles. It is a major breakthrough when mineral crystals were first observed by Zocher [1] in 1925 and since then many reports had focused on inorganic liquid crystal (LC) phase with nanometer-scale objects [2, 3]. Inorganic nanocrystals may be viewed as an emerging new class of macromolecules [4, 5] and enable self-assembly techniques to be extended to inorganic materials, which possesses a diverse range of optical, electrical, and magnetic properties [6]. Many types of inorganic LC phases have already been observed, such as nematic, lamellar, columnar, and spherulites [7–9]. The development of liquid crystal composing of different morphology nanoparticles has been explored, including nanosphere, nanorods, nanodisk, graphene, and nanotubes [10–14], among which the study of rod-shape lyotropic LC behavior is under the spotlight.

The anisotropy of the structural units is necessary for formation of lyotropic LC. Moreover, these units were found to exhibit orientational order in a certain range of concentrations. Recently, the study of oriented nanorods attracts a lot of attention due to its unique properties [15, 16]. There are two basic approaches to the assembly of nanoscale rigid-rod, while the assembly of nanorods (NRs) is necessary for the formation of lyotropic liquid crystals. The first one relies on the Onsager mechanism [17], driving the parallel alignment of NRs when their volume fraction and their aspect ratio are high enough. The second approach utilizes anisotropic attractive forces and thus allows one to produce assembled structures at practically any NRs concentration [18]. The formation of LC phase also offered the potential to orient anisotropic nanoparticles and obtained a large scale of self-assembly superlattic. Some groups had obtained various alignment of anisotropic nanoparticles by self-assembly in liquid crystal, including nanowire [19] and nanorods [20, 21]. Meanwhile oriented NRs self-assembly materials might be obtained by

applying the external field to the LC. Zorn and coworkers had reported on switching behavior under an applied AC (Alternating Current) electric field of ZnO nanorods [22]. In this respect the orientation of functional semiconducting nanoparticles is interesting for materials science [23, 24]. In order to obtain the stable nanorods LC in organic solvent, the particles have to be surface-functionalized to overcome the strong adhesion forces among them and achieve good dispersion [25]. Therefore, the concept of "hairy" rods, which was originally developed for stiff main-chain LCs, is promising [26]. In this model, a stiff insoluble core is solubilized by long alkyl chains (the hairs) on its surface. Other semiconductor NRs were functionalized to give the liquid-crystalline phase in organic solvent, like CdSe [27].

Our group has obtained several self-assembled TiO_2 nanorods structures and tried to study the mechanism of the assembly process [28]. However, some of the critical problems are still waiting to be solved, such as diverse structure of self-assembly and the control of the assembly process. Work presented here introduces a controllable preparation of various TiO_2 NRs structures by a two-step self-assembly, where the NRs were modified by oleic acid (OA). Primary-assembly occurred in synthesis process and two structures were formed, namely, ribbon and honeycomb. Secondary assembly was induced when the products were placed at low temperature. With the increase of concentration, three TiO_2 structures were obtained and these structures showed namatic, spherulite, and lamellar, respectively. We discussed the structures and formation process of unique LC phase, laid emphasis on the growth, properties and possible applications of TiO_2 spherulites in 0.231 M. We also attempted to clarify the main driving force of the two-step assembly process.

2. Experimental Section

Materials. 1-Octadecene (ODE, 90%, Alorich), Oleic acid (OA, 90%, Alfa Aesar), Tetrabutyl titanate (TBT, Chemically Pure, Sinopharm Chemical Reagent). Oleylamine (OLA, 70%, Fluka), n-Hexane (Analytical reagent), Acetone (Analytical reagent, HangZhou Chemical Reagent), and Ethanol (Analytical reagent) were used as received.

Synthesis and Self-Assembly of TiO_2 NRs. Anatase TiO_2 NRs with an elongated *c*-axis were synthesized according to modified literature methods [29]. In a typical synthesis process, OA (3.2 mL, 10 mmol) and 1-ODE (6 mL) were injected into a 50 mL three-neck flask, and the system was kept at 80°C with vigorous stirring for 1 h. TBT (0.48 mL, 2 mmol) was added into the mixed solution, which was heated to 120°C. After 30 min, the solution turned to be yellow, then it was heated to 250–260°C continually. After keeping the solution at 260°C for 10 min, OLA (0.96 mL, 3 mmol) was injected into the mixed solution and the aminolysis reaction was initiated. 90 min later, the resulting solution was allowed to cool to room temperature. All the synthesis process was carried out under argon flow.

Through varying the addition amount of TBT 0.72 mL and 0.96 mL and keeping the molar ratio of TBT : OA : OLA = 2 : 10 : 3, three different NRs solution (0.188 M/0.231 M/0.262 M) were prepared. Then the solution was placed in an incubator at 23°C. About a week, the solution was divided into two layers. The upper layer was yellow supernatant and the lower was gel-like product. The same volume (typical volume was 10 mL) of supernatant liquid was extracted from above solutions and the gel-like products were carried out for the following characterization.

Characterization of Self-Assembly Structures. Powder X-ray diffraction (XRD) patterns were collected on a Philips PW1050 X-ray powder diffractometer with Cu Kα radiation (λ = 1.5406 Å). XRD samples were prepared as follows. After extracting the upper supernatant from the resulting two-layers solution, the lower gel-like products (~5 mL) were dissolved in n-hexane (3 mL). The system was vibrated ultrasonically for 30 min, and then acetone (6 mL) was added into the mixed solution. The crude products were separated in a centrifuge at 5000 rpm and washed with alcohol for several times, and white powder was obtained after drying.

Transmission Electron Microscope (TEM) images were performed with a JEM-1230 TEM operating at accelerating voltages of 80 KV. The samples were prepared by dropping the gel-like products directly on carbon-coated cooper grid and drying in a desiccation.

Polarized Optical Microscope (POM) experiments were operated by a NIKON ECLIPSE E600POL. The samples were prepared by dropping the gel-like products between two slides.

3. Result and Discussion

3.1. Synthesis and Primary-Assembly of Nanorods. We synthesized TiO_2 NRs solution with three different concentrations by keeping the molar ratio of TBT : OA : OLA at 2 : 10 : 3 and varying the amount of TBT, and the concentration of NRs were 0.188 M, 0.231 M, and 0.262 M, respectively (At this point, the volume of TBT was 0.48 mL/0.72 mL/0.96 mL). Figure 1(a) shows typical powder XRD result and TEM image (inset) of the 0.231 M products (other concentrations show similar results), which clearly demonstrates that the products are composed of pure anatase TiO_2 without any other crystalline phase and there is an obvious indication of the crystal growth direction. The [001] diffraction peak exhibits a relatively narrow peak width, which illustrates that the anatase TiO_2 nanorods have a preferred growth orientation along the [001], the *c*-axis direction of the anatase crystal. It can also be proved that the diameter and length of the TiO_2 are 2.3–3.5 nm and 25–30 nm, respectively.

As mentioned before, the final products were obtained after two-step assembly. The primary self-assembly of the TiO_2 nanorods solution occurred spontaneously during the synthesis process [30], and two structures (ribbon and honeycomb) were obtained. Ribbon structure (Figure 1(a), inset) was assembled through side-by-side attraction of NRs to 0.1–1 μm, and honeycomb (Figure 2(a)) is a high packing density structure consisting of perpendicularly aligned rods in hexagonal superlattic. After the sample was kept at 21–25°C

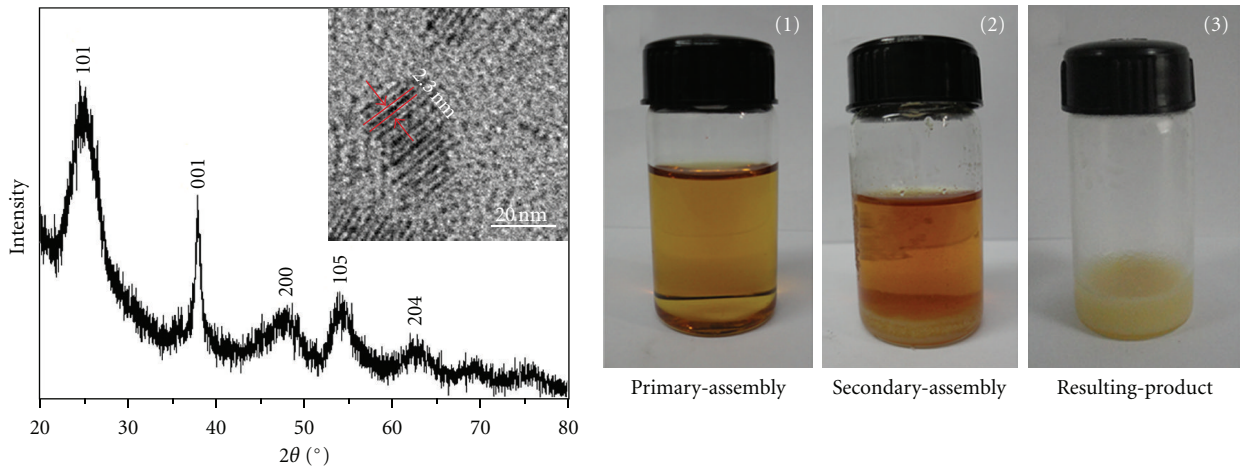

FIGURE 1: (a) The XRD pattern of anatase TiO_2 nanorods and corresponding TEM image (inset). (b) The products after primary and secondary assembly, and resulting gel-like products.

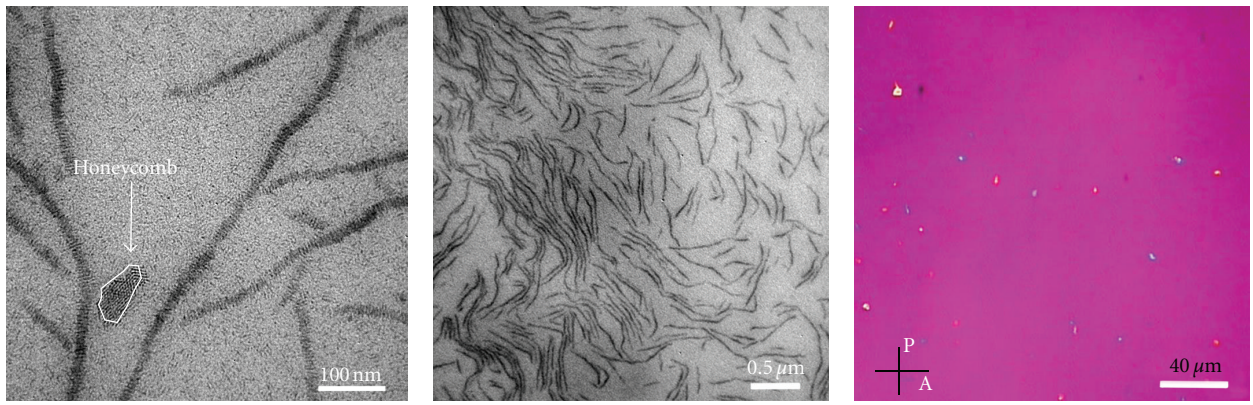

FIGURE 2: (a, b) TEM images of 0.188 M products after synthesis and being placed one week. (c) POM image of 0.188 M.

(accelerate the secondary assembly and avoid solidification of oleic acid, typical temperature is 23°C) for about one week, the secondary self-assembly will be induced. Although the aspect ratio of NRs is consistent, unique structure is obtained at different concentrations after the secondary assembly. The liquid crystal behavior of each structure was characterized and will be discussed in the next section. Primary-assembly structures are used as the building units of the subsequent secondary self-assembly [31] at this time. The formation of liquid crystalline phases of TiO_2 NRs solution is verified by an optical microscope with crossed polarizer, while the self-assembly structure is characterized by TEM. The products at 0.231 M after primary and secondary assembly are shown in Figure 1(b), Figure 1(b) (3) is the gel-like products after extracting the supernatant from the NRs solution (other concentrations show the same phenomenon).

3.2. Secondary Self-Assembly and LC Phases on Increasing Concentration. The following discussion will focus on the structures and properties of LC phases after secondary assembly at different concentrations. The possible reason for those differences is that the relative amount of two secondary building units (ribbon and honeycomb). As shown in Figure 2(a), at low NRs concentration such as 0.188 M, both structures' concentrations are too low to trigger the secondary assembly, so the secondary-assembly process does not happen. Moreover, the amount of ribbon structure is still much more than honeycomb (Figure 2(b)), and they will enrich and form nematic phase after being placed for a week. The corresponding POM image (Figure 2(c)) also shows a typical nematic texture.

It is worth mentioning that the aggregates in 0.231 M show a Maltese-cross extinction pattern under polarizing microscope (Figure 3(c)), which indicates that they form spherulites structure. It also can be found that the first and third quadrants are yellow, while the second and fourth quadrants are blue in spherulites texture, inferring that we obtain negative or tangential spherulites [32, 33] whose

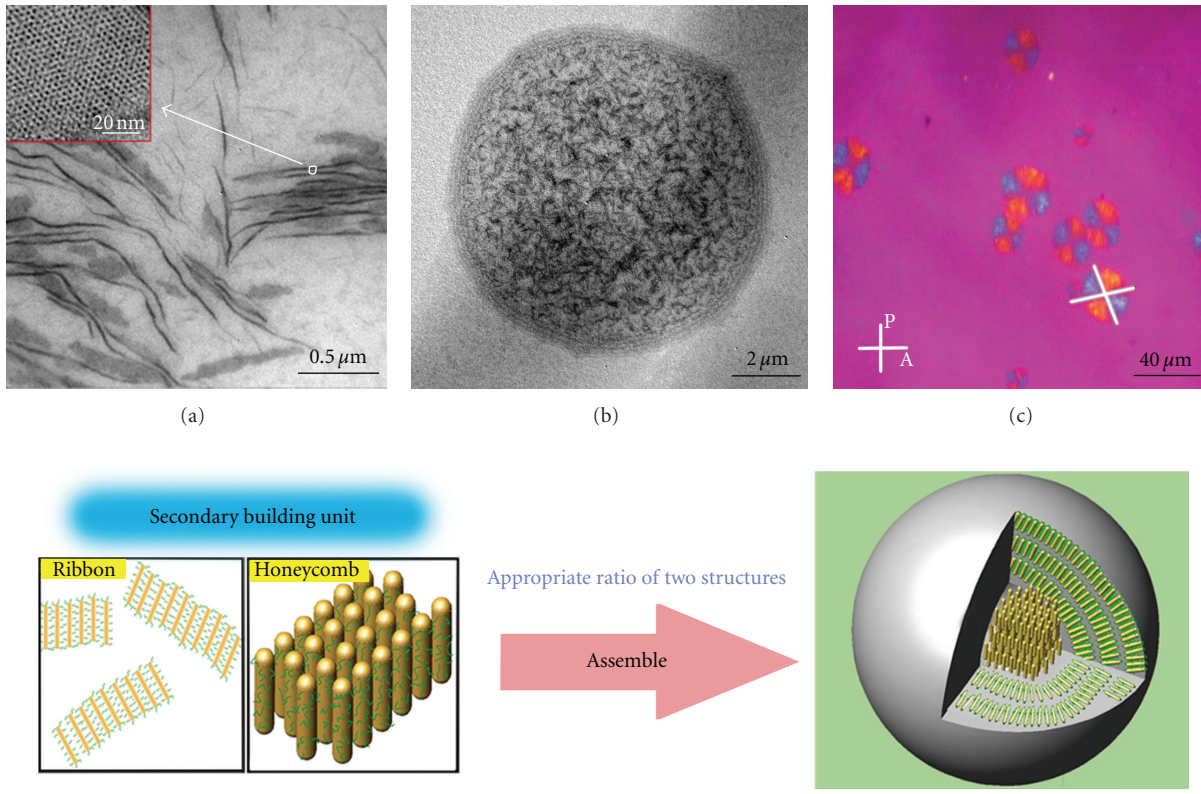

Figure 3: (a) TEM image of structures when primary assembly of TiO_2 NRs was complete; inset is the honeycomb structure. (b) TEM image of spherulite after secondary assembly at 0.231 M. (c) POM image of spherulites of anatase TiO_2. (d) The schematic illustration for the formation of spherulites.

crystallites are suggested to lie along the circumference. Figure 3(a) shows a representative TEM image of the products after primary assembly, as the secondary building unit, it is obvious that the amount of honeycomb is almost equal to that of ribbon structure and its diameter is more than two hundreds nanometer. The assembly is completely different from the aggregation of NRs in 0.188 M; this time the secondary-assembly occurred. The honeycomb becomes the key factor, because it was used as nuclei to induce nucleation when its content and diameter reach the threshold. After that, the ribbon structure assembles along the circumference of nuclei and grows into spherulites with dozens or even hundreds of microns in diameter under certain temperature. Figure 3(b) shows a TEM image of not so perfect TiO_2 spherulite whose structure is consistent with the theory and experiments. Figure 3(d) shows the schematic illustration of the formation of spherulites. This is the first report about spherulites formed from anatase TiO_2 NRs, although other systems are known to have formed spherulites, including organic material [34, 35] and inorganic CdSe nanorods [36].

The growth processes of TiO_2 nanorods spherulite at 0.231 M were determined by examining different time at an appropriate temperature. According to a series of experiments, the most suitable temperature for the formation of spherulites is 23°C (other range of temperatures will form subperfect spherulites). Figures 4(a)–4(e) show the POM images of the growth of NRs spherulites at 23°C. Apparently the growth process starts from the center, while many of the honeycomb structures assemble gradually, which forms the spherulites core of hundreds of nanometer, and then the nanoribbons continue to assemble around the core along the circumferential direction to form 20–30 μm spherulites. As shown in Figure 4(f), a well-defined Maltese cross was observed and the TiO_2 nanorods spherulites formed have the opposite negative-type crystal structure.

A series of other experiments about temperature range in which spherulite can exist have been carried out for the applications. The initial temperature was 23°C, and both the heating and cooling rates were set at 1°C/min and maintained for 5 min at every testing temperature (to prevent errors because of the slow growth of spherulites and there is no other changes happen given more time). The spherulites disappeared when the temperature reached 30°C and re-appeared when they were cooled down to 26–28°C (Figure 5), but the spherulites have a high chemical stability at a certain temperature. According to features of spherulites, we can develop a kind of temperature microsensor, which works under 23–40°C. Of course the operating temperature range can be regulated by the NRs concentrations, solvent types, or other factors. Based on the growth process, spherulites also may be used in drug detoxification [37].

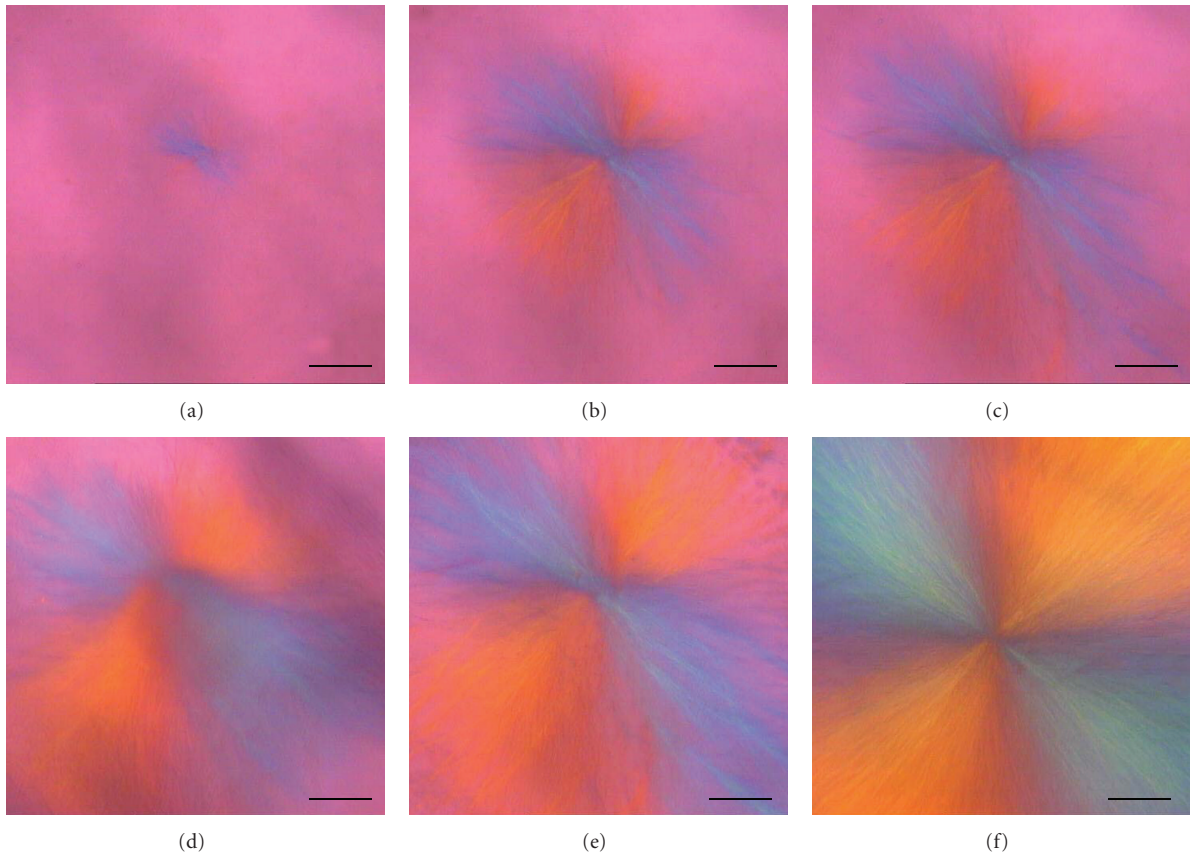

Figure 4: (a–e) Images of the growth process of spherulites from nucleation under crossed polarizing microscope. (f) Representative POM image of spherulites and a Maltese-cross extinction pattern. All scale bars are 5 μm.

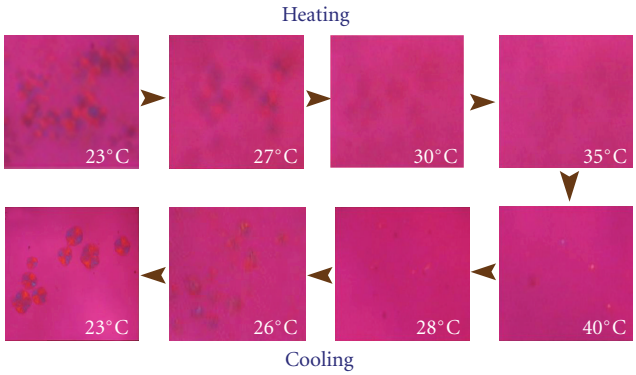

Figure 5: The influence of temperature variation to the spherulites under crossed polarizing microscope.

When the concentration increases to 0.262 M, the NRs solution will assemble into lamellar (or smectic) phase which is a more ordered, lower energy of lyotropic liquid crystal phase. Figure 6(a) shows a typical TEM image after the primary self-assembly, which demonstrates that there is no sign of honeycomb structure. As the amount of TiO_2 ribbon structure is very high, it is arranged in a perfect layer structure by end-by-end contact type, and the distance between the layer is approximately twice of the length of surface ligands of the NRs (Figure 6(b)). This is a novel method to obtain an ordered array of nanorods via regulation of lyotropic liquid crystal. Figure 6(c) is a corresponding POM image at 0.262 M, which also reveals a typical texture of smectic phase. Figure 6(d) shows schematic illustration for the formation of lamellar phase.

3.3. Assembly Mechanism and the Driving Force. Based on the TEM and POM experimental observations, the process and self-assembly mechanism of the NRs is hypothesized (Figures 3(d) and 6(d)). The final products were obtained by a two-step assembly, that is, primary and secondary self-assembly. In the synthesis process, the primary assembly occurred and formed two structures named as ribbon and honeycomb, respectively. These two structures appeared in various concentrations, including the lowest one, which is lower than what is needed to satisfy the Onsager theory. Those facts reveal that the main driving force for primary-assembly should be the anisotropic attractive force and thus allow the NRs to assemble at any concentrations. Only ribbon structure is found at high NRs concentration, and the most possible reason is that higher concentrations means wider size distribution, so the NRs intend to form ribbon structure, which is less ordered than the honeycomb. We explain the assembly by Van der Waals attraction between surface ligands of the TiO_2 NRs. Because the affinity of

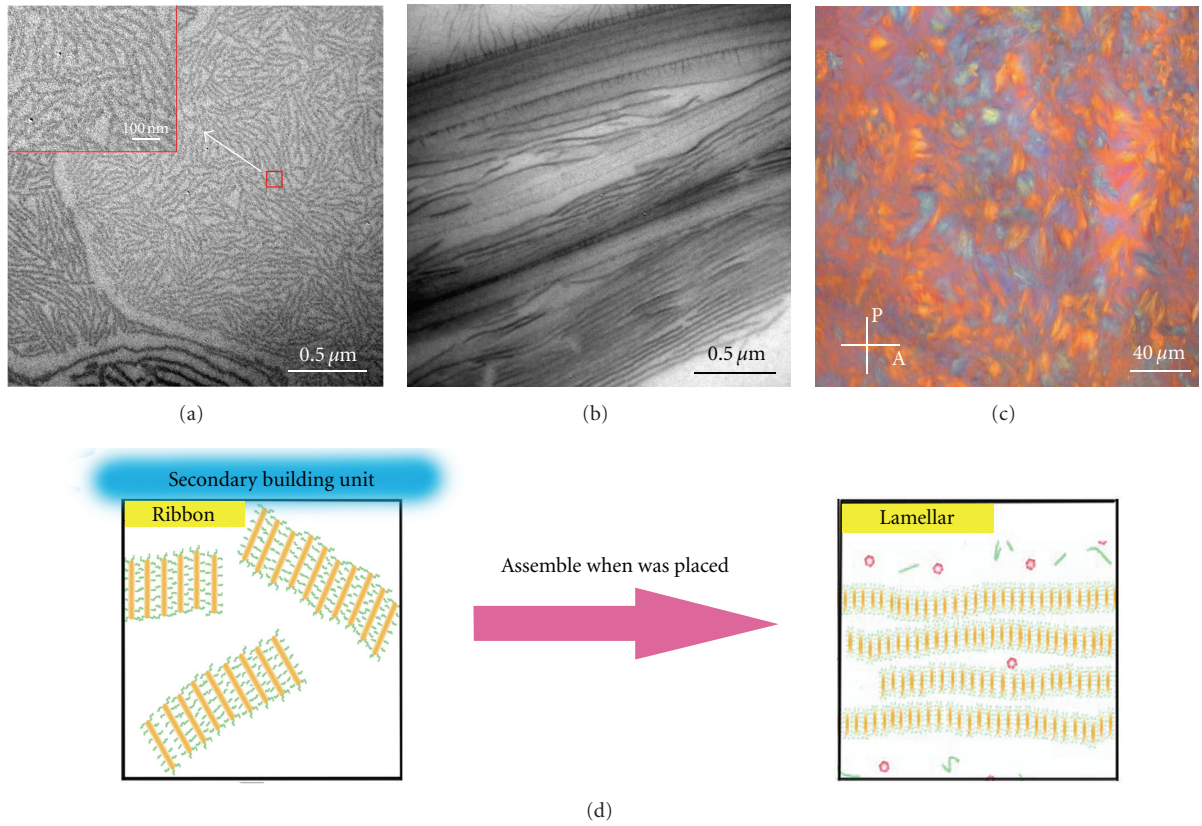

Figure 6: (a) TEM image of the 0.262 M TiO_2 NRs solution after primary assembly. (b) TEM image of lamellar phase after secondary assembly. (c) POM image of lamellar phase. (d) Schematic illustration for the formation of lamellar.

OA for the lateral surfaces of NRs is higher than that for the end facet, the Van der Waals attraction among laterals is more powerful, which makes rods form side-by-side structure. Meanwhile, the repulsion force will increase with the decrease of distance between the NRs to keep system in balance. In the case of having closer parameters and uniform aspect ratio, the NRs form honeycomb structure to decrease the interfacial energy effectively, because honeycomb is more compact compared with ribbon. The multilayer honeycomb can be obtained as the pairing of the dipole moment along the longitudinal by the antiparallel [38] of NRs, while the two ends whose polarity is opposite cannot be infinitely close to each other because the free H^+ will be absorbed to the negative end, thus the system is also in equilibrium. As long as the major forces for this process are the intermolecular/colloidal forces, further assembly is possible as secondary and tertiary self-assembly [31]. When the product was placed at 21–25°C for about one week, secondary self-assembly occurred. The main driving force for this assembly is gravity. Several structures are formed because the relative amount of honeycomb and ribbon structures is different at various concentrations. The enrichment of ribbon structure causes the formation of nematic phase in 0.188 M. Each structure shows unique LC behavior after secondary-assembly, namely, nematic, spherulite, and lamellar on increasing concentration (see Figures 2, 3, and 6).

4. Conclusion

In conclusion, various TiO_2 NRs structures were obtained by a two-step self-assembly. In primary assembly occurring in the synthesis process, two structures appeared, that is, ribbon and honeycomb, respectively. However, the relative amount of these two structures is different at various concentrations: only a small amount of both two structures were found in 0.188 M, approximately equal amount of honeycomb and ribbon were found in 0.231 M, and only ribbon appeared in 0.262 M concentration. Since these two structures obtained by primary assembly were used as the secondary building unit and the amount of them are different, we obtained three secondary assembly structures after secondary assembly with the increase of concentration. Each structure has unique LC behavior. We investigate the growth process of spherulites and conceive the possible applications such as spherulites in temperature microsensor and drug detoxification. The mechanism of the two-step self-assembly was clarified. Further experiments will be carried out to characterize the behavior and properties of TiO_2 nanorods LC for its possible applications.

Acknowledgments

The authors gratefully acknowledge the financial support for this work from the National Natural Science Foundation of

China (nos. 50928201, 50972127, and 51010002), the Fundamental Research Funds for the Central Universities and the Zhejiang Provincial Natural Science Foundation of China (nos. Z4080021 and Y4090067), and the Doctoral Fund of the Ministry of Education of China (no. 20100101110039).

References

[1] H. Zocher, "Über freiwillige Strukturbildung in Solen. (Eine neue Art anisotrop flüssiger Medien.)," *Zeitschrift für Anorganische und Allgemeine Chemie*, vol. 147, no. 1, pp. 91–110, 1925.

[2] J. C. P. Gabriel and P. Davidson, "New trends in colloidal liquid crystals based on mineral moieties," *Advanced Materials*, vol. 12, no. 1, pp. 9–20, 2000.

[3] S. Saliba, Y. Coppel, P. Davidson et al., "Liquid crystal based on hybrid zinc oxide nanoparticles," *Journal of Materials Chemistry*, vol. 21, no. 19, pp. 6821–6823, 2011.

[4] C. Robinson and J. C. Ward, "Liquid-crystalline structures in polypeptides," *Nature*, vol. 180, no. 4596, pp. 1183–1184, 1957.

[5] C. Park, J. Lee, and C. Kim, "Functional supramolecular assemblies derived from dendritic building blocks," *Chemical Communications*, vol. 47, pp. 12042–12056, 2011.

[6] A. P. Alivisatos, "Semiconductor clusters, nanocrystals, and quantum dots," *Science*, vol. 271, no. 5251, pp. 933–937, 1996.

[7] S. Meuer, P. Oberle, P. Theato, W. Tremel, and R. Zentel, "Liquid crystalline phases from polymer-functionalized TiO_2 nanorods," *Advanced Materials*, vol. 19, no. 16, pp. 2073–2078, 2007.

[8] G. J. Vroege, D. M. E. Thies-Weesie, A. V. Petukhov, B. J. Lemaire, and P. Davidson, "Smectic liquid-crystalline order in suspensions of highly polydisperse goethite nanorods," *Advanced Materials*, vol. 18, no. 19, pp. 2565–2568, 2006.

[9] M. Wojcik, W. Lewandowski, J. Matraszek et al., "Liquid-crystalline phases made of gold nanoparticles," *Angewandte Chemie*, vol. 48, no. 28, pp. 5167–5169, 2009.

[10] Z. Shen, M. Yamada, and M. Miyake, "Control of stripelike and hexagonal self-assembly of gold nanoparticles by the tuning of interactions between triphenylene ligands," *Journal of the American Chemical Society*, vol. 129, no. 46, pp. 14271–14280, 2007.

[11] L. L. Yang, Q. X. Zhao, M. Willander, X. J. Liu, M. Fahlman, and J. H. Yang, "Effective suppression of surface recombination in ZnO nanorods arrays during the growth process," *Crystal Growth & Design*, vol. 10, no. 4, pp. 1904–1910, 2010.

[12] A. E. Saunders, A. Ghezelbash, D. M. Smilgies, M. B. Sigman Jr., and B. A. Korgel, "Columnar self-assembly of colloidal nanodisks," *Nano Letters*, vol. 6, no. 12, pp. 2959–2963, 2006.

[13] Z. Xu and Z. Gao, "Aqueous liquid crystals of graphene oxide," *ACS Nano*, vol. 5, no. 4, pp. 2908–2915, 2011.

[14] Y. S. Kwon, B. M. Jung, H. Lee, and J. Y. Chang, "Preparation of polymeric SWNT—liquid crystal composites using a polymerizable surfactant," *Macromolecules*, vol. 43, no. 12, pp. 5376–5381, 2010.

[15] X. Liu, W. Zhou, Z. Yin, X. Hao, Y. Wu, and X. Xu, "Growth of single-crystalline rutile TiO_2 nanorod arrays on GaN light-emitting diodes with enhanced light extraction," *Journal of Materials Chemistry*, vol. 22, pp. 3916–3921, 2012.

[16] L. Gong, X. Wu, H. Chen, F. Qu, and M. An, "Synthesis of vertically aligned dense ZnO nanowires," *Journal of Nanomaterials*, vol. 2011, Article ID 428172, 5 pages, 2011.

[17] L. Onsager, "The effects of shape on the interaction of colloidal particles," *Annals of the New York Academy of Sciences*, vol. 51, pp. 627–659, 1949.

[18] H. S. Park, A. Agarwal, N. A. Kotov, and O. D. Lavrentovich, "Controllable side-by-side and end-to-end assembly of Au nanorods by lyotropic chromonic materials," *Langmuir*, vol. 24, no. 24, pp. 13833–13837, 2008.

[19] S. Zhang, P. W. Majewski, G. Keskar, L. D. Pfefferle, and C. O. Osuji, "Lyotropic self-assembly of high-aspect-ratio semiconductor nanowires of single-crystal ZnO," *Langmuir*, vol. 27, no. 18, pp. 11616–11621, 2011.

[20] D. F. Gardner, J. S. Evans, and I. I. Smalyukh, "Towards reconfigurable optical metamaterials: colloidal nanoparticle self-assembly and self-alignment in liquid crystals," *Molecular Crystals and Liquid Crystals*, vol. 545, no. 1, pp. 3/[1227]–21/[1245], 2011.

[21] A. A. Ezhov, G. A. Shandryuk, G. N. Bondarenko et al., "Liquid-crystalline polymer composites with CdS nanorods: structure and optical properties," *Langmuir*, vol. 27, no. 21, pp. 13353–13360, 2011.

[22] M. Zorn, M. N. Tahir, B. Bergmann et al., "Orientation and dynamics of ZnO nanorod liquid crystals in electric fields," *Macromolecular Rapid Communications*, vol. 31, no. 12, pp. 1101–1107, 2010.

[23] M. Schierhorn, S. W. Boettcher, J. H. Peet et al., "CdSe nanorods dominate photocurrent of hybrid CdSe-P3HT photovoltaic cell," *ACS Nano*, vol. 4, no. 10, pp. 6132–6136, 2010.

[24] L. Baeten, B. Conings, H. G. Boyen et al., "Towards efficient hybrid solar cells based on fully polymer infiltrated ZnO nanorod arrays," *Advanced Materials*, vol. 23, no. 25, pp. 2802–2805, 2011.

[25] M. N. Tahir, N. Zink, M. Eberhardt et al., "Overcoming the insolubility of molybdenum disulfide nanoparticles through a high degree of sidewall functionalization using polymeric chelating ligands," *Angewandte Chemie*, vol. 45, no. 29, pp. 4809–4815, 2006.

[26] M. Ballauff, "Stiff-chain polymers—structure, phase behavior, and properties," *Angewandte Chemie*, vol. 28, no. 3, pp. 253–267, 1989.

[27] L. S. Li, J. Walda, L. Manna, and A. P. Alivisatos, "Semiconductor nanorod liquid crystals," *Nano Letters*, vol. 2, no. 6, pp. 557–560, 2002.

[28] B. Ye, G. D. Qian, X. P. Fan, and Z. Y. Wang, "Self-assembled superlattices from colloidal TiO_2 nanorods," *Current Nanoscience*, vol. 6, no. 3, pp. 262–268, 2010.

[29] Z. Zhang, X. Zhong, S. Liu, D. Li, and M. Han, "Aminolysis route to monodisperse titania nanorods with tunable aspect ratio," *Angewandte Chemie*, vol. 44, no. 22, pp. 3466–3470, 2005.

[30] Z. Y. Huo, C. K. Tsung, W. Y. Huang et al., "Self-organized ultrathin oxide nanocrystals," *Nano Letters*, vol. 9, no. 3, pp. 1260–1264, 2009.

[31] Y. S. Lee, *Self-Assembly and Nanotechnology: A Force Balance Approach*, John Wiley & Sons, Hoboken, NJ, USA, 2008.

[32] S. Kobayashi, L. J. Hobson, J. Sakamoto et al., "Formation and structure of artificial cellulose spherulites via enzymatic polymerization," *Biomacromolecules*, vol. 1, no. 2, pp. 168–173, 2000.

[33] S. B. Murray and A. C. Neville, "The role of the electrostatic coat in the formation of cholesteric liquid crystal spherulites from α-chitin," *International Journal of Biological Macromolecules*, vol. 20, no. 2, pp. 123–130, 1997.

[34] D. C. Bassett, "Polymer spherulites: a modern assessment," *Journal of Macromolecular Science B*, vol. 42, no. 2, pp. 227–256, 2003.

[35] J. H. Magill, "Review spherulites: a personal perspective," *Journal of Materials Science*, vol. 36, no. 13, pp. 3143–3164, 2001.

[36] D. V. Talapin, E. V. Shevchenko, C. B. Murray, A. Kornowski, S. Föraster, and H. Weller, "CdSe and CdSe/CdS nanorod solids," *Journal of the American Chemical Society*, vol. 126, no. 40, pp. 12984–12988, 2004.

[37] A. B. Dhanikula, M. Lafleur, and J. C. Leroux, "Characterization and in vitro evaluation of spherulites as sequestering vesicles with potential application in drug detoxification," *Biochimica et Biophysica Acta*, vol. 1758, no. 11, pp. 1787–1796, 2006.

[38] S. C. McGrother, A. Gil-Villegas, and G. Jackson, "The effect of dipolar interactions on the liquid crystalline phase transitions of hard spherocylinders with central longitudinal dipoles," *Molecular Physics*, vol. 95, no. 3, pp. 657–673, 1998.